



Real-time observations of stable isotope dynamics during rainfall and throughfall events

Barbara Herbstritt, Benjamin Gralher, Markus Weiler

Hydrology, Faculty of Environment and Natural Resources, Albert-Ludwigs-University, Freiburg, 79098, Germany

5 *Correspondence to:* Barbara Herbstritt (barbara.herbstritt@hydrology.uni-freiburg.de)

Abstract. The isotopic composition of throughfall is affected by complex exchange, enrichment, and mixing processes in the tree canopy. All interception processes occur simultaneously in space and time generating a complex pattern of throughfall in amount and isotopic composition. This pattern ultimately cascades through the entire hydrologic system and is therefore crucial for studies in catchment hydrology where recharge areas are often forested while reference meteorological stations are generally in the open. For the quasi real-time observation of the isotopic composition of both gross precipitation and throughfall we developed an approach combining an off-the-shelf membrane contactor (Membrana) with a laser-based Cavity Ring-Down Spectrometer (CRDS, Picarro), obtaining isotope readings every two seconds. For the continuous observation of the temporal effect of interception processes two setups with two CRDS instruments in parallel were used analysing gross precipitation and throughfall simultaneously. All devices were kept small to minimize dead volume and thereby, with time-lags of only four minutes, to increase the temporal resolution of isotope observations. Complementarily, meteorological variables were recorded in high temporal resolution at the same location. Comparing these high temporally resolved continuous measurements with discrete liquid or event-based bulk samples, this approach proves to be a powerful tool towards more insight in the very dynamic processes contributing to interception during rainfall events.

10
15

1 Introduction

20 Stable isotope signatures of water ($\delta^{18}\text{O}$ and $\delta^2\text{H}$) are ideal tracers due to the fact that they are part of the water molecule itself (Gonfiantini, 1986). They have proven to be powerful tools in hydrology with a long record of applications at different spatial and temporal scales and in all parts of the water cycle. The isotopic composition of precipitation ultimately cascades through the entire hydrologic system affecting soil water, groundwater, evapotranspiration, and stream water isotopic signatures and is therefore crucial for studies in catchment hydrology. There are extensive reviews of stable isotope applications in catchment hydrology (Kendall and McDonnell, 1998; Vitvar et al., 2005). Many studies have used the temporal dynamics in the isotopic composition of precipitation for estimating residence times, but especially in forested catchments interception losses and accompanying isotope effects play an important role (Xu et al., 2014; Stockinger et al., 2015; Allen et al., 2017), since recharge areas are often forested whereas meteorological and isotopic reference stations are generally in the open. The importance of understanding rainfall interception processes is presented in a thorough review by

25



(Allen et al., 2017). The reasons for the differences in amount and isotopic composition of gross precipitation (P_g) and throughfall (TF) are complex, since multiple interacting processes affect TF. They are driven by evaporation from the canopy during or between storms, isotopic exchange with ambient vapour, redistribution in the canopy, and storage effects where water is differentially retained or mixed. Also sub-canopy water recycling i.e. evapotranspiration and re-condensation (Green et al., 2015) as well as mixing with water from previous events (Allen et al., 2014) has been described. These effects reduced the mean amount of weekly sampled TF compared to P_g . Depending on the type (spruce and beech) and density of the vegetation cover in a range of 12% to 41% (Brodersen et al., 2000) the interception loss has typically been higher for small events and generally leading to isotopic enrichment of TF. However, ignoring the differences between P_g and TF results in an overestimation of the input amount to the system and is therefore a source of error in hydrograph separation (Kubota and Tsuboyama, 2004). In ungauged catchments or when only P_g instead of TF data is available, isotopic correction factors were determined empirically (Stockinger et al., 2015; Calderon and Uhlenbrook, 2016) serving as surrogates to compensate for the lack of respective TF isotope data.

Typically high spatial intra- and inter-storm variabilities have been found in amount and isotopic composition. In a synthesis study analysing the spatiotemporal variabilities of TF from 18 selected studies at a global scale, it was found that their spatial patterns related to leaf area index (LAI) as well as to spatial variability in general, were very heterogeneous and ecosystem dependent (Levia, 2011). Another study used a set of 94 gauges at three different forested sites, covering different species and ages of trees, canopy densities and canopy diameters. They investigated the spatial dependence of TF amount with a geostatistical approach finding a high temporal persistence (Keim et al., 2005). Recently, the observation of high spatial variability in collected TF stable isotopic compositions could be improved by using a set of roving collectors (Allen et al., 2015). Although hypothesized, intra- and inter-storm variabilities of TF amount did not necessarily correspond with variations in isotopic composition. Consequently, collecting representative TF input data is still missing and an observational challenge.

Traditionally, the isotopic composition of liquid water is determined with discrete samples being analysed in the laboratory, hence conducting isotope studies always implied a trade-off between limited spatio-temporal resolution and extensive (and expensive) lab work. With the recent development of laser-based isotope analysers like off-axis integrated cavity output spectroscopy (OA-ICOS) or Cavity Ring-Down Spectroscopy (CRDS), there is now the possibility to analyse water stable isotopes faster and less expensive. The fact that water vapour is analysed directly ‘as water’ together with the field-deployability of the analysers and the virtually instant availability of isotope readings made way for several attempts aiming at in-situ isotope observations with high temporal resolutions. Berman et al. (2009) and Pangle et al. (2013) combined an autosampler with a flow-through system and were able to reveal otherwise unnoticed fine-scale (5-minutes) variations of precipitation isotopic compositions. A commercially available VALCO[®] valve unit coupled with laser spectrometers for high-resolution sampling (9.5-minutes) was used by Leis et al. (2011) to investigate spring water isotope dynamics. Koehler and Wassenaar (2011) employed a marble-filled equilibrator and a minimodule device for producing and subsequently analysing a constant stream of vapour being in isotopic equilibrium with and therefore carrying in a known manner the



isotopic information of the liquid phase of interest. Following the same principle, other researchers used gas-permeable ePTFE surgical tubings for the investigation of precipitation trajectories (Munksgaard et al., 2012b) or seawater-freshwater mixing ratios (Munksgaard et al., 2012a). For the continuous investigation of rapid isotope changes in a soil column experiment, Herbstritt et al. (2012) employed a commercially available hydrophobic membrane contactor for converting a small fraction of liquid water continuously into a stream of vapour, which was directly analysed by the coupled isotope analyser. However, none of these approaches have attempted to observe rainfall and throughfall in parallel.

Recent interception studies, mostly based on bulk sampling data and focusing on spatial variations, are especially lacking an appropriate temporal resolution to be comparable with the available temporal resolution of meteorological input data and hence to describe and better understand the physics controlling the differences in isotopic composition between P_g and TF.

Therefore, the aim of this study is to develop an approach for P_g and TF analysis at high temporal resolution based on the membrane contactor method, to compare and validate the continuous isotope measurements with discrete liquid samples as well as with event-based bulk samples. With this approach the dynamics in amount and isotopic composition of P_g and TF and hence, interception processes influencing amount and isotopic composition of TF can be investigated in high temporal resolution.

15

2 Methods and Material

2.1 Sampling

We modified the setup developed and used previously for the in situ observation of water stable isotopes in a soil column experiment (Herbstritt et al, 2012). A commercially available hydrophobic membrane contactor of 1 x 1 x 0.5 inch (MicroModule[®], Membrana, Charlotte, NC, USA, www.liquicel.com) was combined with a CRDS isotope analyser (L2120-*i*, Picarro, Inc., Santa Clara, CA, USA, www.picarro.com). The contactor, originally designed for degassing liquids, was used in the so called ‘sweep-mode’ in order to continuously transform a small fraction of liquid water of interest with flowrates of 5-30 mL/min, according to manufacturer specifications, into a water vapour stream. Inside the contactor a microporous, hydrophobic, PP-based membrane ($A=100\text{cm}^2$) divides the liquid from the gaseous phase. At the membrane’s surface, dry carrier gas (e.g. N_2) mixes with vapour evolving from the liquid water flowing through the contactor and moist air leaves the contactor at the gas outlet port (Fig. 1, right) which is directly connected to the CRDS. In the analyser-controlled stream of moist air (flow rate $\sim 35\text{mL/min}$), readings of water vapour, $\delta^{18}\text{O}$ and $\delta^2\text{H}$ are given every two seconds. The method requires a thorough determination of the temperature to account for the temperature-dependent isotope fractionation factors of the membrane as described in detail by Herbstritt et al. (2012).

Several modifications of the original setup were made for the quasi real-time observation of stable water isotopes in rainfall. A standard rainfall collector was enlarged from 200 to 1810 cm^2 with a PP-funnel to ensure sufficient water flow in case of low rainfall intensities and also to account for small-scale spatial variabilities in TF, when measured below the canopy. To



protect against litter fall, a metal mesh with 1 x 1 mm covered the funnel. At the bottom end a smaller funnel with a volume of 3 mL was installed. From there, a stream of water was pumped to the membrane contactor with a peristaltic pump at a constant flowrate of 5 mL/min while at the same time water exceeding this flowrate was spilled, contributing to the event-based bulk sample.

- 5 All connections were made by gas-tight PFA tubings with an inner diameter of 1 mm. Easily replaceable glass fibre syringe filters (pore size 1-2 μ m) were installed in line to protect the membrane contactor from clogging. Removal of smaller particles or biofilms inside the contactor could be facilitated by periodical back flushing with deionized water or rinsing with weak acids, respectively. Temperature of the water in the tubing just before the contactor was stabilized and kept constant at 16°C using a peltier element (UEPT-KIT3) and a controller (UR3274U5, both obtained from uwe electronic, Wachendorf,
- 10 Germany, www.uweelectronic.de) to avoid super-saturation and condensation of the vapour on the way to the isotope analyser operated at room temperature. Vapour isotope data were recorded as soon as temperature and thus vapour concentration at the membrane contactor was stable, which was usually the case within 5 to 10 minutes after the onset of precipitation sampling. All tubings were kept as short as possible, facilitating a time shift of no more than four minutes between precipitation and the respective readings displayed by the isotope analyser (Fig. 1). During rainfall events, discrete
- 15 liquid samples were taken every five minutes at the liquid outlet port of the membrane module, the collected overflow plus excess water at the membrane module was volume-weighted and summed up to an event-based bulk sample. In close proximity (1.5 m) to each collector a tipping bucket (R3, Onset Rain Gauge) was installed. Rainfall was logged in 0.2 mm increments (HOBO UA-003-64 Pendant Event Data Logger, Onset, HOBO[®], Bourne, MA, USA, www.onsetcomp.com) and data was aggregated to 1-minute intervals. Two of these setups were installed 10 m apart, sampling gross precipitation (P_g)
- 20 and throughfall (TF) separately under a deciduous tree (*acer campestre*) in the vegetation period (May-September) of 2016. The meteorological variables air temperature (T_a) and relative humidity (RH) were recorded in 15 m distance to the tree with a CS215 sensor and logged with a CR1000 data logger (both available from Campbell Scientific, Inc., Logan, UT, USA, www.campbellsci.com) every minute. Additionally, the meteorological variables rainfall amount (P_g), air temperature (T_a), relative humidity (RH), air pressure, wind speed (v), maximum wind speed (v_{max}), and wind direction were available in 10
- 25 minute resolution from a climate station 250 m away.

Figure 1

30 2.2 Analyses

All isotope data are expressed in δ -notation calculated following Eq. (1):



$$\delta = \left(\frac{R_{sample}}{R_{VSMOW}} - 1 \right) * 1000\text{‰} \quad (1)$$

where VSMOW is the Vienna Standard Mean Ocean Water and R is the isotope ratio ($^{18}\text{O}/^{16}\text{O}$ or $^2\text{H}/^1\text{H}$). Calibration of the samples was conducted using three in-house standards with distinct isotopic composition (-16.65‰, -9.59‰, and 0.51‰ for $\delta^{18}\text{O}$, -125.05‰, -66.50‰, and -2.40‰ for $\delta^2\text{H}$), referenced to the international VSMOW-SLAP scale (Craig, 1961). They were pumped consecutively through the contactor after each rainfall event and treated similar to the continuously sampled precipitation water. Hence, potential long-term changes of the membranes did not have an effect on calibrated isotope data. For data noise reduction of the continuous measurements we calculated moving averages with an integration time of 90 s.

All liquid water samples were analysed on a CRDS laser spectrometer (Picarro L2130-*i*) with a post-calibration accuracy of $\pm 0.053\text{‰}$ for $\delta^{18}\text{O}$ and $\pm 0.349\text{‰}$ for $\delta^2\text{H}$.

D-excess (d) was used to indicate deviation from the global meteoric water line (GMWL) and likely non-equilibrium fractionation by evaporation (Gat, 1996):

$$d = \delta^2\text{H} - 8 * \delta^{18}\text{O} \quad (2)$$

The difference $\text{TF} - \text{P}_g$ is indicated by the symbol Δ :

$$\Delta\delta^{18}\text{O} = \delta^{18}\text{O}_{\text{TF}} - \delta^{18}\text{O}_{\text{Pg}} \quad (3)$$

$$\Delta d = d_{\text{TF}} - d_{\text{Pg}} \quad (4)$$

Vapour pressure deficit $E-e$ is calculated with the following equation (modified from Foken, 2008):

$$E - e = 6.107\text{hPa} * e^{\left(\frac{17.62 * T_a}{243.12 + T_a}\right)} * \left(1 - \frac{RH}{100}\right) \quad (5)$$

where RH is relative humidity in % and T_a is air temperature in °C.

3 Results

One example rainfall event observed in this study started with high rainfall intensities followed by more moderate intensities which lasted for roughly two hours. Continuous vapour stable isotope measurements, liquid grab and liquid bulk samples are shown for both isotope ratios investigated to illustrate the increase of temporal information during one single rain event when sampling in high temporal resolution (Fig. 2). The moving average of calibrated vapour data ranged between -5.45‰ and -7.53‰ (-27.36‰ and -45.64‰) for $\delta^{18}\text{O}$ ($\delta^2\text{H}$) with a mean precision of $\pm 0.26\text{‰}$ ($\pm 1.53\text{‰}$). Calibrated data of the liquid samples taken simultaneously were in a range of -5.34‰ to -7.43‰ in the case of $\delta^{18}\text{O}$ and -28.73‰ to -45.95‰ in the case of $\delta^2\text{H}$. Mean absolute deviation between the continuously measured vapour data and the discrete liquid samples was 0.13‰ ($\delta^{18}\text{O}$) and 1.12‰ ($\delta^2\text{H}$). The isotopic composition of the three-hour bulk sample during this event was -5.68‰ and -32.67‰ for $\delta^{18}\text{O}$ and $\delta^2\text{H}$, respectively.



Figure 2

Analysing all event-based bulk samples in this study, the variables rainfall amount (P_g), mean rainfall intensity, interception loss, the difference in deuterium excess (Δd) and the isotopic difference $\Delta\delta^{18}\text{O}$ were compared in a scatterplot matrix (Fig. 3). In the upper right part the respective Pearson correlation coefficient is shown, indicating a significant (p -value < 0.05) negative correlation between the logarithm of rainfall intensity and interception loss indicating that the highest interception losses were found during events with lowest rainfall intensities (Fig. 3a). Predominantly the interception loss ranged between 30 and 50%. Also a positive correlation between $\Delta\delta^{18}\text{O}$ (the difference in $\delta^{18}\text{O}$ between P_g and TF) and interception loss was found (Fig. 3b) which means that $\delta^{18}\text{O}$ was stronger altered in throughfall when interception losses are high.

10

Figure 3

For bulk samples (Fig. 4, right), a maximum of 2 - 2.5‰ was found in $\Delta\delta^{18}\text{O}$ values only for a few events, while for most events $\Delta\delta^{18}\text{O}$ was 1.5‰ or less. In contrast, in the shorter periods of continuous sampling $\Delta\delta^{18}\text{O}$ values up to 3.5‰ were found (Fig. 4, left). In the left part of this figure each symbol indicates the mean $\Delta\delta^{18}\text{O}$ (y-axis), whereas the length of the symbols indicate the duration (x-axis) including start and end time of the respective events. Two clusters could be identified where one contained single rainfall events on a previously dry canopy, whereas the other was generated by events on already wet canopies with markedly higher $\Delta\delta^{18}\text{O}$ values.

20 Figure 4

Time series of a) $\Delta\delta^{18}\text{O}$, b) $\Delta\delta^2\text{H}$, and c) Δd calculated from continuous isotope data of TF and P_g of all events observed are illustrated in Figure 5. Values during events on dry canopy did not exceed 1.5‰ (10‰) for $\Delta\delta^{18}\text{O}$ ($\Delta\delta^2\text{H}$) with Δd values ranging from +1 to -7, while values from events on wet canopy were in the range of +1.5 to +5‰ (11 to 43‰) for $\Delta\delta^{18}\text{O}$ ($\Delta\delta^2\text{H}$) with Δd values ranging from +12 to -6 ‰.

Figure 5

The combination of collector funnel area (1810 cm³) and water flow rate (5 mL/min) resulted in a threshold rainfall intensity of 0.03 mm/min that was required to ensure an air bubble-free stream of water being pumped to the membrane contactor. Thus, periods of continuous water flow at both (P_g and TF) contactors alternated with periods when air bubbles appeared at either one or both of the contactors in this example event (Fig. 6). Since the presence of bubbles proved to flaw isotope readings, calculations of $\Delta\delta^{18}\text{O}$, $\Delta\delta^2\text{H}$, and Δd were only possible for periods with bubbles at neither contactor. The



variability of the continuous P_g isotope data is higher than that of the continuous TF data where the signal is more dampened over time. Relative to P_g , TF becomes increasingly enriched in heavy isotopes during the event. Air temperature as well as vapour pressure deficit become lower with event duration, while at the same time mixing of canopy-stored water with “fresh” precipitation water has to be assumed.

5

Figure 6

4 Discussion

The modified setup of the method developed by Herbstritt et al. (2012) adapted to continuous rainfall and throughfall isotope measurement worked quite well in terms of providing continuous, thermo-regulated flows of water to the membrane modules and delivering reliable liquid water stable isotope data. The latter became evident by the good agreement of continuous measurements and single liquid samples (Fig. 2 and Fig. 6). Large inter-storm variabilities exist in the isotopic signature of P_g and TF, which were impossible to detect when solely relying on commonly taken event-based bulk samples or even on data representing a higher sampling interval of typically 5mm precipitation. The dynamics in the isotopic composition in P_g as well as in TF could nicely be captured by the continuous measurements and also to some degree with the 5-minute liquid grab samples. Due to required minimum flowrates at the contactor (5 mL/min), the used setup with a collector area of 1810 cm² was limited to minimum rainfall intensities of 0.03 mm/min (1.8 mm/h). For intensities below the identified threshold value, a larger or multiple collectors would be necessary, whereby larger collection funnels in combination with low rainfall intensities will increase the risk of evaporative enrichment from the funnel leading to methodological artefacts that need to be avoided. Therefore, dimensioning the collectors always is a trade-off and the maximum size is limited.

In the collected bulk samples significant correlations between interception loss and meteorological variables like rainfall amount or intensity could be observed (Fig. 3), as expected. There is no clear pattern for only one of these variables, which is evidence for the complexity of processes contributing to interception loss and the transformation of P_g isotope ratios when becoming TF. Comparing $\Delta\delta^{18}\text{O}$ data during continuously measured events with those of event-based bulk samples, the differences are larger during the shorter continuously measured periods (Fig. 4). Furthermore, two clusters could be distinguished representing rainfall on already wet and on initially dry canopies (Fig. 4 left). This allows for the interpretation that antecedent conditions have a clear impact on isotopic enrichment of TF. The total number of observed events is lower in the case of the continuously measured events due to a number of events with rainfall intensities below the threshold for the continuous sampling method and due to several events during the night when the sampling setup was not operated. For continuous measurements the differences in the isotopic signature were consistently calculated from isochronic P_g and TF data although we are aware that water falling from the canopy (i.e. TF) is always a mixture of new rainfall (i.e. isochronic P_g) and rainfall that has fallen at different points in time before. The time lags depend on canopy storage capacity and rainfall



intensity (Allen, 2017) and therefore vary within each single event as well as between different storms. Associating TF to P_g of the same point in time is therefore only partly correct.

Relative to P_g , TF becomes increasingly enriched in heavy isotopes (Fig. 6), which is similar to our observations of $\Delta\delta^{18}\text{O}$ in bulk samples on dry and wet canopies (Fig. 4 and Fig. 5). Meteorological variables did not provide a clear single evidence for this enrichment, indicating that multiple variables take effect. Typically, air temperature as well as vapour pressure deficit slightly decreased over the course of an event, but probably evaporation still took place. At the same time mixing with fresh precipitation water still occurred. Therefore, it remains unclear to what extent the increase in difference between synchronous P_g and TF isotope data must be attributed to evaporative enrichment or to changing mixing processes following the variable rainfall intensities. In addition, the spatial scale of mixing, probably at the leaf level, but also among leaves resulting from water dripping from leaf to leaf, needs to be considered if we would like to simulate the isotope dynamics caused by water mixing and evaporation in the canopy of a tree.

5 Conclusions

We could demonstrate that the proposed method is suitable for continuously observing the stable water isotope dynamics in precipitation and throughfall at the plot level. We facilitated a huge increase in temporal resolution compared to isotope assays based on discrete sampling. Our approach supersedes taking liquid samples and at the same time provides data much faster. The instant data availability enables immediate reactions during rainfall events while the operator is still in the field. Employing our setup, the temporal resolution of the isotope data corresponds with the temporal resolutions that are already common in high frequency meteorological observations.

All components employed in this study are commercially available and can be installed with reasonable effort. In the present design the setup cannot yet be left unattended due to the necessity of periodical cleaning and maintenance like changes of the in-line filters. However, proper precautions excluding clogging by e.g. leaf debris should solve this issue as well. We are therefore confident that this study will contribute to the aim of thorough isotopic sampling of TF which is crucial in hydrological studies on forested sites as pointed out repeatedly (Keim et al., 2005; Stockinger et al., 2015; Allen et al., 2017).

Due to the selected setup dimensions and the resulting minimum rainfall intensity of 0.03 mm/min in this study, the system was not able to capture events with low intensities, e.g. most stratiform rainfall events. Furthermore, knowledge about intra-canopy mixing and the time lags between P_g and TF as required for a precise, physically based calculation of the evaporative enrichment still remains a challenge for future applications.



Acknowledgements

We gratefully thank our technician Emil Blattmann for technical assistance. The article processing charge was funded by the German Research Foundation (DFG) and the University of Freiburg in the funding programme Open Access Publishing.

5

References

- Allen, S. T., Brooks, J. R., Keim, R. F., Bond, B. J., and McDonnell, J. J.: The role of pre-event canopy storage in throughfall and stemflow by using isotopic tracers, *Ecohydrology* 7, doi: 10.1002/eco.1408, 2014
- Allen, S. T., Keim, R. F., Barnard, H. R., McDonnell, J. J., and Renée Brooks, J.: The role of stable isotopes in understanding rainfall interception processes: a review, *Wiley Interdiscip Rev Water* 4, e1187. doi: 10.1002/wat2.1187, 2017
- Allen, S. T., Keim, R. F., and McDonnell, J. J.: Spatial patterns of throughfall isotopic composition at the event and seasonal timescales, *J Hydrol* 522, 58–66, doi: 10.1016/j.jhydrol.2014.12.029, 2015
- Berman, E. S. F., Gupta, M., Gabrielli, C., Garland, T., and McDonnell, J. J.: High-frequency field-deployable isotope analyzer for hydrological applications, *Water Resour Res* 45, W10201, doi: 10.1029/2009wr008265, 2009
- Brodersen, C., Pohl, S., Lindenlaub, M., Leibundgut, C., and Wilpert, K. v.: Influence of vegetation structure on isotope content of throughfall and soil water, *Hydrol Process* 14, 1439–1448, doi: 10.1002/1099-1085(20000615)14:8<1439::AID-HYP985>3.0.CO;2-3, 2000
- Calderon, H. and Uhlenbrook, S.: Characterizing the climatic water balance dynamics and different runoff components in a poorly gauged tropical forested catchment, Nicaragua, *Hydrol Sci J* 61, 2465–2480, doi: 10.1080/02626667.2014.964244, 2016
- Craig, H.: Standards for reporting concentrations of deuterium and oxygen-18 in natural waters, *Science* 133, 3467, 1961
- Foken, T.: *Micrometeorology*, Springer-Verlag, doi: 10.1007/978-3-540-74666-9, 2008
- Gat, J. R.: Oxygen and hydrogen isotopes in the hydrologic cycle, *Annu Rev Earth Planet Sci* 24, 225–262, doi: 10.1146/annurev.earth.24.1.225, 1996
- Gonfiantini, R.: Environmental Isotopes in Lake Studies, in: Fontes J.-Ch. and Fritz, P. (eds.): *Handbook of Environmental Isotope Geochemistry*, Elsevier, Amsterdam, 113–168, 1986
- Green, M. B., Laursen, B. K., Campbell, J. L., McGuire, K. J., and Kelsey, E. P.: Stable water isotopes suggest sub-canopy water recycling in a northern forested catchment, *Hydrol Process* 29, 5193–5202, doi: 10.1002/hyp.10706, 2015
- Herbstritt, B., Gralher, B., and Weiler, M.: Continuous in situ measurements of stable isotopes in liquid water. *Water Resour Res* 48:W03601, doi: 10.1029/2011wr011369, 2012
- 30



- Keim, R. F., Skaugset, A. E., and Weiler, M.: Temporal persistence of spatial patterns in throughfall, *J Hydrol* 314, 263–274, doi: <https://doi.org/10.1016/j.jhydrol.2005.03.021>, 2005
- Kendall, C. and McDonnell, J. J.: *Isotope tracers in catchment hydrology*, Elsevier Science, Amsterdam, New York, 1998
- 5 Koehler, G. and Wassenaar, L. I.: Realtime Stable Isotope Monitoring of Natural Waters by Parallel-Flow Laser Spectroscopy, *Anal Chem* 83, 913–919, doi: 10.1021/ac102584q, 2011
- Kubota, T. and Tsuboyama, Y.: Estimation of evaporation rate from the forest floor using oxygen-18 and deuterium compositions of throughfall and stream water during a non-storm runoff period, *J For Res* 9, 51–59, doi: 10.1007/s10310-003-0054-y, 2004
- 10 Leis, A., Plieschnegger, M., Harum, T., Stadler, H., Schmitt, R., Pelt, A.v., and Zerobin, W.: Isotope Investigations at an Alpine Karst Aquifer by Means of On-Site Measurements with High Time Resolution and Near Real-Time Data Availability, in: *International Symposium in Isotopes in Hydrology, Marine Ecosystems and Climate Change Studies*, 2011
- Levia, D. F., Keim, R.F., Carlyle-Moses, D.E., and Frost, E.E.: Throughfall and Stemflow in Wooded Ecosystems, in: *Forest Hydrology and Biogeochemistry*, Springer-Verlag, 425-443, 2011
- 15 Munksgaard, N. C., Wurster, C. M., Bass, A., Zagorskis, I., and Bird, M. I.: First continuous shipboard $\delta^{18}\text{O}$ and δD measurements in sea water by diffusion sampling-cavity ring-down spectrometry, *Environ Chem Lett* 10, 301–307, doi: 10.1007/s10311-012-0371-5, 2012a
- Munksgaard, N. C., Wurster, C. M., Bass, A., and Bird, M. I.: Extreme short-term stable isotope variability revealed by continuous rainwater analysis, *Hydrol Process* 26, 3630–3634, doi: 10.1002/hyp.9505, 2012b
- 20 Pangle, L. A., Klaus, J., Berman, E. S. F., Gupta, M., and McDonnell, J. J.: A new multisource and high-frequency approach to measuring $\delta^{2}\text{H}$ and $\delta^{18}\text{O}$ in hydrological field studies, *Water Resour Res* 49, 1-7, doi: 10.1002/2013wr013743, 2013
- 25 Stockinger, M. P., Lücke, A., McDonnell, J. J., Diekkrüger, B., Vereecken, H., and Bogena, H. R.: Interception effects on stable isotope driven streamwater transit time estimates, *Geophys Res Lett* 42, 5299–5308, doi: 10.1002/2015GL064622, 2015
- Vitvar, T., Aggarwal, P., and McDonnell, J. J.: A Review of Isotope Applications in Catchment Hydrology, in: Aggarwal P., Gat J. R., Froehlich K. F. (eds.): *Isotopes in the Water Cycle*, Springer, Dordrecht, 2005
- Xu, X., Guan, H., and Deng, Z.: Isotopic composition of throughfall in pine plantation and native eucalyptus forest in South Australia, *J Hydrol* 514, 150–157, doi: <http://dx.doi.org/10.1016/j.jhydrol.2014.03.068>, 2014

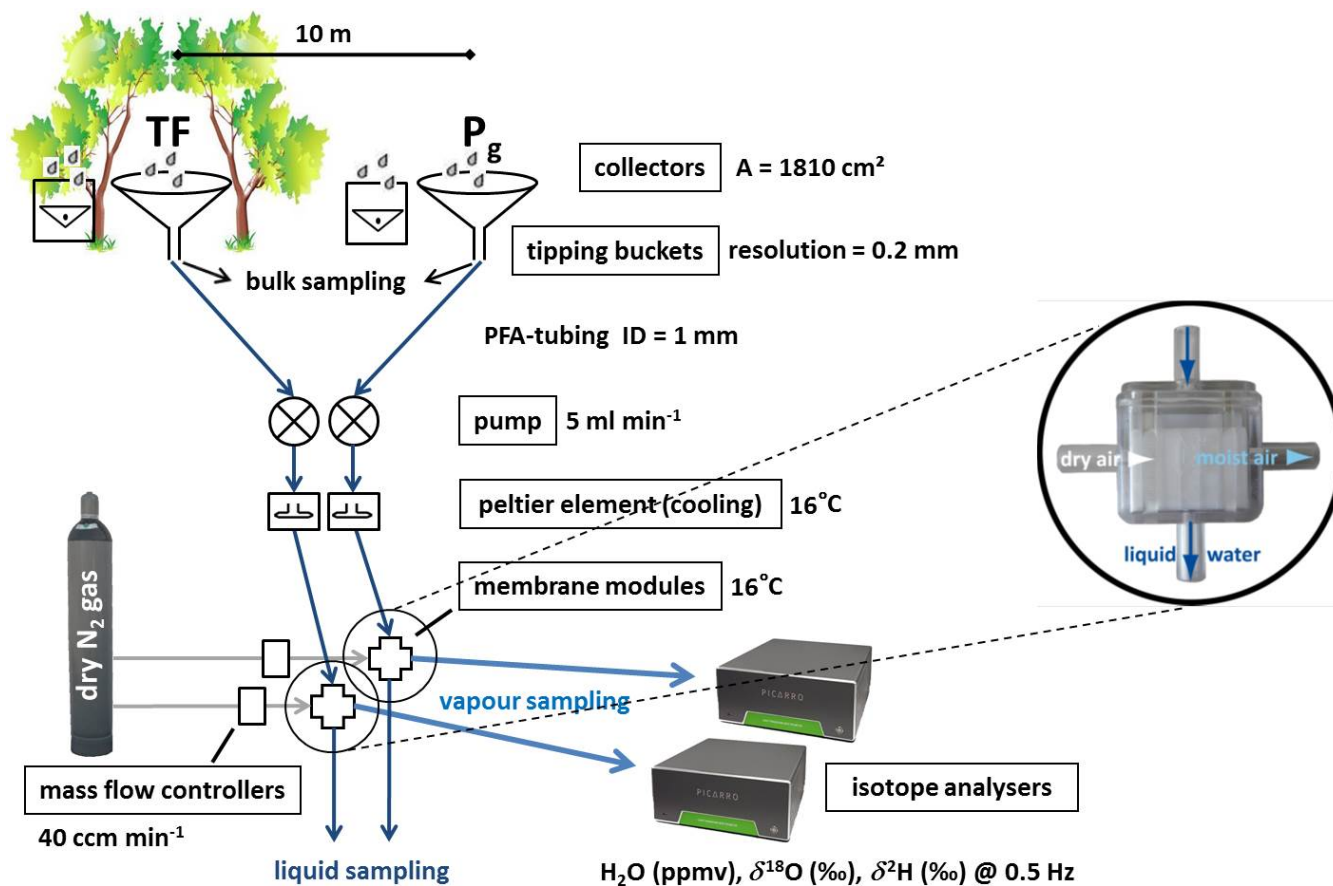


Figure 1: Setup for continuous vapour stable isotope measurements, liquid grab and bulk sampling of gross precipitation (P_g) and throughfall (TF); right: membrane contactor employed for converting liquid water into water vapour.

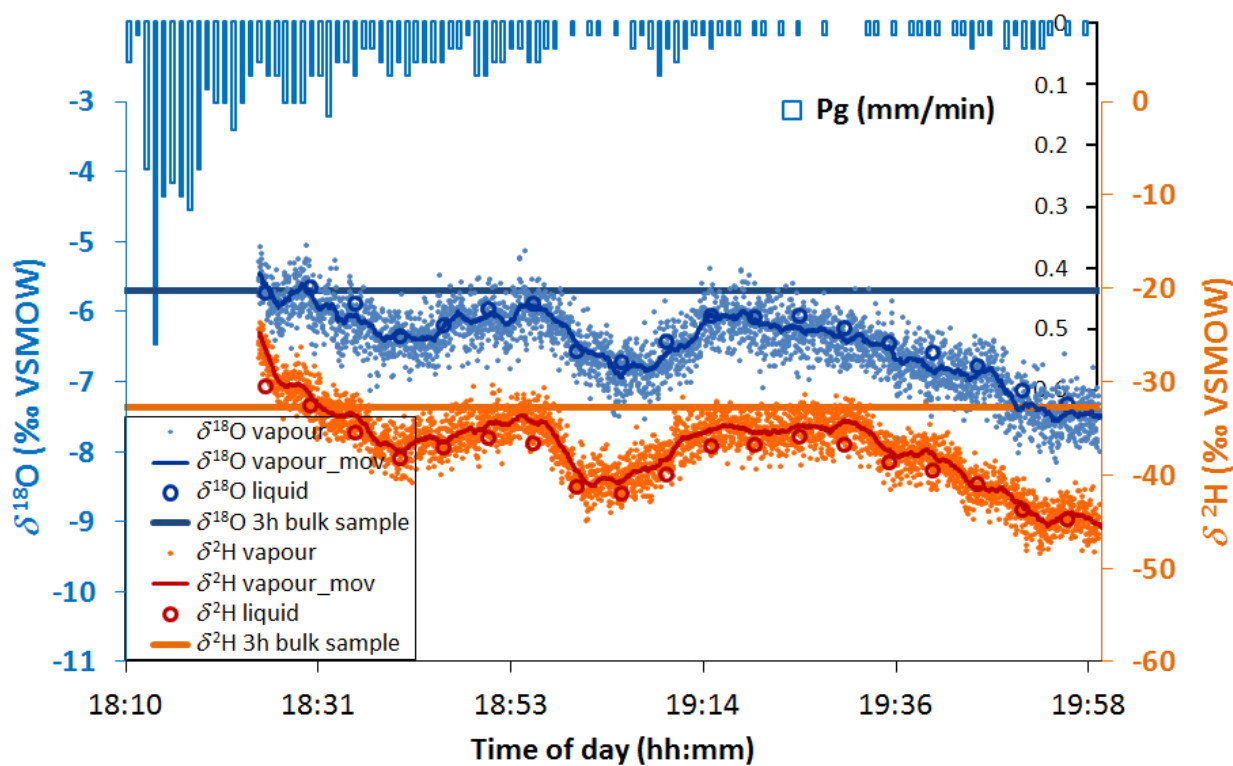


Figure 2: Time series of rainfall per minute (vertical bars) during one example rainfall event; data of $\delta^{18}\text{O}$ in blue and $\delta^2\text{H}$ in red; vapour data recorded every two seconds (small dots), 90 sec. moving average (thin lines), liquid grab samples (big circles) taken every five minutes, three-hour bulk sample (horizontal bars).

5

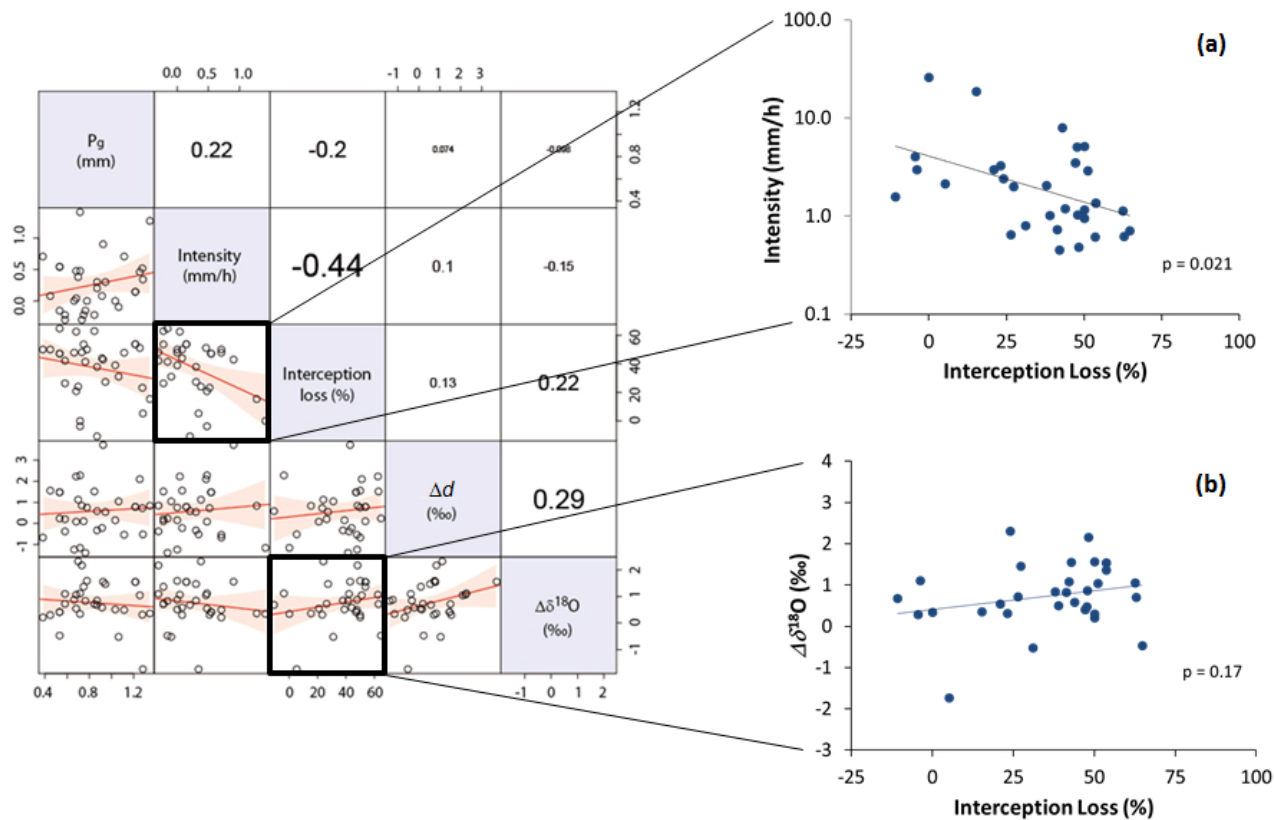


Figure 3: Scatter plot matrix of bulk samples in throughfall. a) Correlation between rainfall intensity and interception loss of bulk samples; b) Correlation between $\Delta\delta^{18}O$ and interception loss of bulk samples.

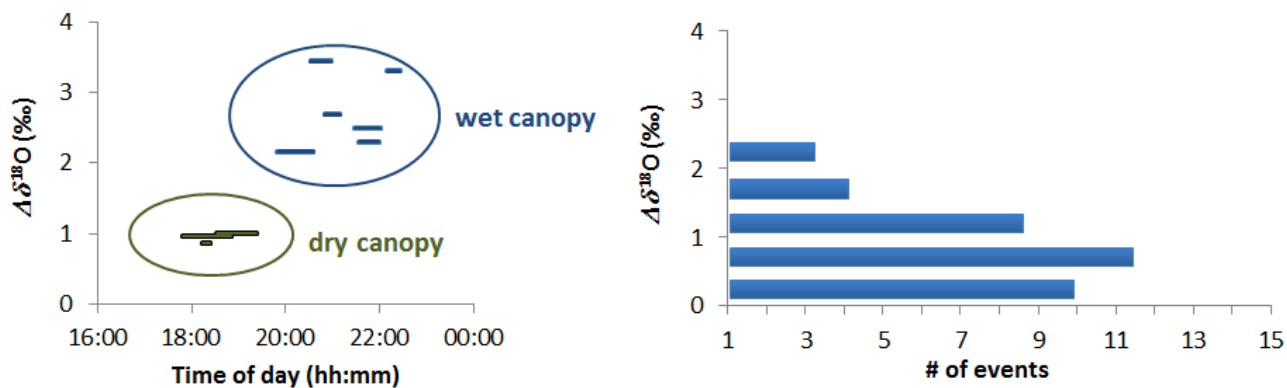
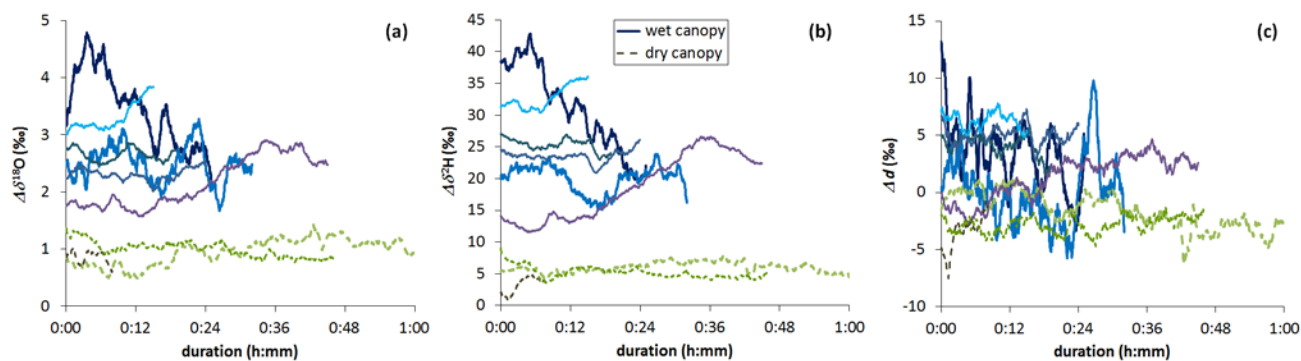


Figure 4: Deviation of the isotopic signature ($\Delta\delta^{18}\text{O}$) between TF and P_g for continuously analysed events (left) and event-based bulk samples of the same period (right).



5 **Figure 5: Time series of deviation of isotopic signature between TF and P_g , a) $\Delta\delta^{18}\text{O}$, b) $\Delta\delta^2\text{H}$, c) Δd . Dashed lines: events on previously dry canopy, solid lines on wet canopy.**

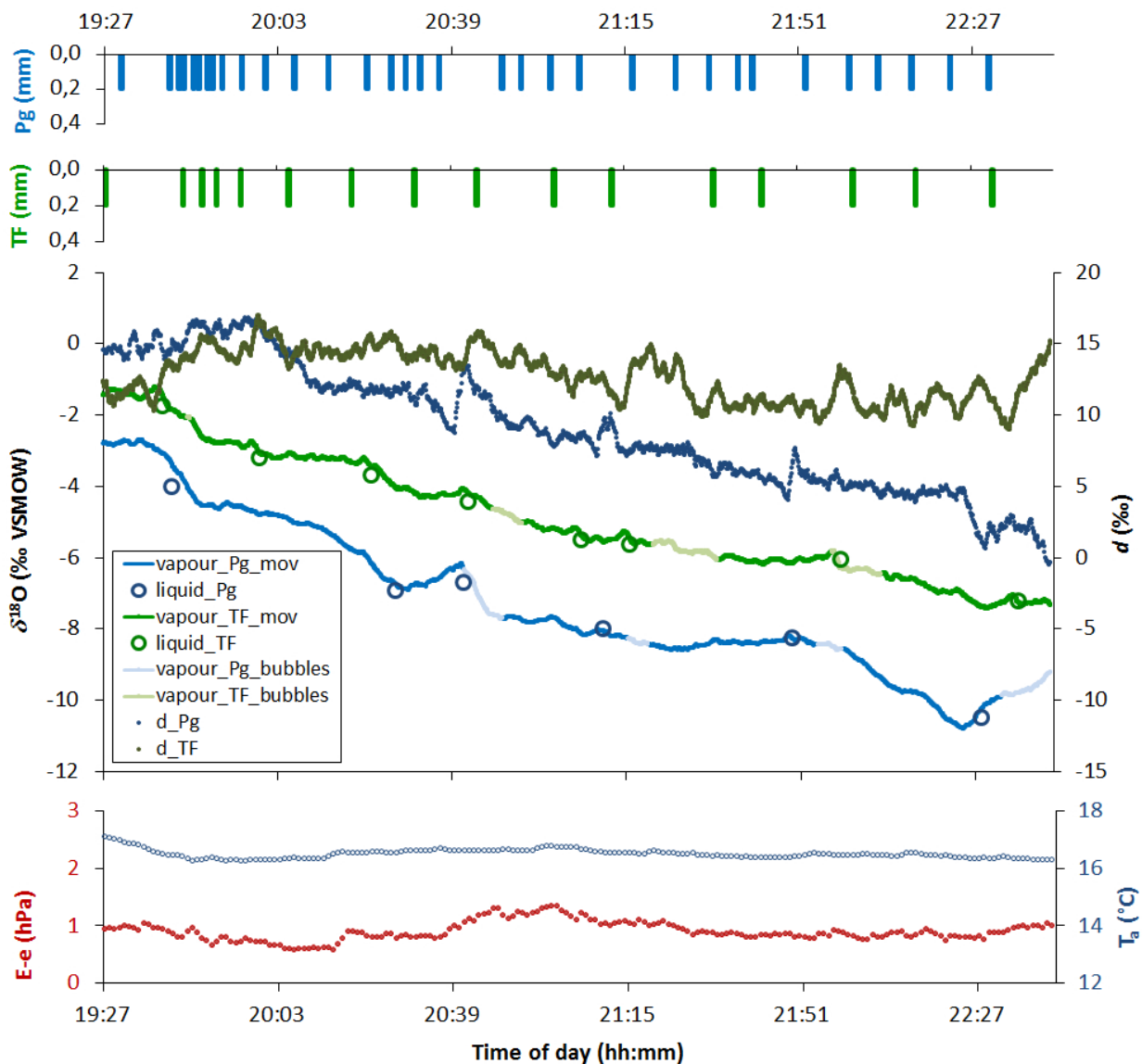


Figure 6: Timeseries of amounts, $\delta^{18}\text{O}$ and d in vapour of P_g (blue) and TF (green), discrete liquid samples (big circles), air temperature (T_a) (small blue circles) and vapour pressure deficit (E-e) (red). Time series of d and T_a are referenced on the right vertical axes. Periods of intensities below threshold for the continuous sampling method (bubbles at membrane contactor) are shown in light blue (P_g) and light green (TF).